

J/ψ production at high transverse momenta in *p+p* and Cu+Cu collisions at $\sqrt{s_{\text{NN}}} = 200$ GeV

B. I. Abelev,⁸ M. M. Aggarwal,³⁰ Z. Ahammed,⁴⁷ B. D. Anderson,¹⁸ D. Arkhipkin,¹² G. S. Averichev,¹¹ J. Balewski,²² O. Barannikova,⁸ L. S. Barnby,² J. Baudot,¹⁶ S. Baumgart,⁵² D. R. Beavis,³ R. Bellwied,⁵⁰ F. Benedosso,²⁷ M. J. Betancourt,²² R. R. Betts,⁸ A. Bhasin,¹⁷ A. K. Bhati,³⁰ H. Bichsel,⁴⁹ J. Bielcik,¹⁰ J. Bielcikova,¹⁰ B. Biritz,⁶ L. C. Bland,³ M. Bombara,² B. E. Bonner,³⁶ M. Botje,²⁷ J. Bouchet,¹⁸ E. Braidot,²⁷ A. V. Brandin,²⁵ E. Bruna,⁵² S. Bueltmann,²⁹ T. P. Burton,² M. Bystersky,¹⁰ X. Z. Cai,⁴⁰ H. Caines,⁵² M. Calderón de la Barca Sánchez,⁵ O. Catu,⁵² D. Cebra,⁵ R. Cendejas,⁶ M. C. Cervantes,⁴² Z. Chajecski,²⁸ P. Chaloupka,¹⁰ S. Chattopadhyay,⁴⁷ H. F. Chen,³⁸ J. H. Chen,¹⁸ J. Y. Chen,⁵¹ J. Cheng,⁴⁴ M. Cherney,⁹ A. Chikanian,⁵² K. E. Choi,³⁴ W. Christie,³ R. F. Clarke,⁴² M. J. M. Codrington,⁴² R. Corliss,²² T. M. Cormier,⁵⁰ M. R. Cosentino,³⁷ J. G. Cramer,⁴⁹ H. J. Crawford,⁴ D. Das,⁵ S. Dash,¹³ M. Daugherty,⁴³ L. C. De Silva,⁵⁰ T. G. Dedovich,¹¹ M. DePhillips,³ A. A. Derevschikov,³² R. Derradi de Souza,⁷ L. Didenko,³ P. Djawotho,⁴² S. M. Dogra,¹⁷ X. Dong,²¹ J. L. Drachenberg,⁴² J. E. Draper,⁵ J. C. Dunlop,³ M. R. Dutta Mazumdar,⁴⁷ W. R. Edwards,²¹ L. G. Efimov,¹¹ E. Elhalhuli,² M. Elnimr,⁵⁰ V. Emelianov,²⁵ J. Engelage,⁴ G. Eppley,³⁶ B. Erazmus,⁴¹ M. Estienne,⁴¹ L. Eun,³¹ P. Fachini,³ R. Fatemi,¹⁹ J. Fedorisin,¹¹ A. Feng,⁵¹ P. Filip,¹² E. Finch,⁵² V. Fine,³ Y. Fisyak,³ C. A. Gagliardi,⁴² L. Gaillard,² D. R. Gangadharan,⁶ M. S. Ganti,⁴⁷ E. J. Garcia-Solis,⁸ A. Geromitsos,⁴¹ F. Geurts,³⁶ V. Ghazikhanian,⁶ P. Ghosh,⁴⁷ Y. N. Gorbunov,⁹ A. Gordon,³ O. Grebenyuk,²¹ D. Grosnick,⁴⁶ B. Grube,³⁴ S. M. Guertin,⁶ K. S. F. F. Guimaraes,³⁷ A. Gupta,¹⁷ N. Gupta,¹⁷ W. Guryan,³ B. Haag,⁵ T. J. Hallman,³ A. Hamed,⁴² J. W. Harris,⁵² W. He,¹⁵ M. Heinz,⁵² S. Heppelmann,³¹ B. Hippolyte,¹⁶ A. Hirsch,³³ E. Hjort,²¹ A. M. Hoffman,²² G. W. Hoffmann,⁴³ D. J. Hofman,⁸ R. S. Hollis,⁸ H. Z. Huang,⁶ T. J. Humanic,²⁸ L. Huo,⁴² G. Igo,⁶ A. Iordanova,⁸ P. Jacobs,²¹ W. W. Jacobs,¹⁵ P. Jakl,¹⁰ C. Jena,¹³ F. Jin,⁴⁰ C. L. Jones,²² P. G. Jones,² J. Joseph,¹⁸ E. G. Judd,⁴ S. Kabana,⁴¹ K. Kajimoto,⁴³ K. Kang,⁴⁴ J. Kapitan,¹⁰ D. Keane,¹⁸ A. Kechechyan,¹¹ D. Kettler,⁴⁹ V. Yu. Khodyrev,³² D. P. Kikola,²¹ J. Kiryluk,²¹ A. Kisiel,²⁸ S. R. Klein,²¹ A. G. Knospe,⁵² A. Kocoloski,²² D. D. Koetke,⁴⁶ M. Kopytine,¹⁸ W. Korsch,¹⁹ L. Kotchenda,²⁵ V. Kouchpil,¹⁰ P. Kravtsov,²⁵ V. I. Kravtsov,³² K. Krueger,¹ M. Krus,¹⁰ C. Kuhn,¹⁶ L. Kumar,³⁰ P. Kurnadi,⁶ M. A. C. Lamont,³ J. M. Landgraf,³ S. LaPointe,⁵⁰ J. Lauret,³ A. Lebedev,³ R. Lednicky,¹² C-H. Lee,³⁴ J. H. Lee,³ W. Leight,²² M. J. LeVine,³ C. Li,³⁸ N. Li,⁵¹ Y. Li,⁴⁴ G. Lin,⁵² S. J. Lindenbaum,²⁶ M. A. Lisa,²⁸ F. Liu,⁵¹ J. Liu,³⁶ L. Liu,⁵¹ T. Ljubicic,³ W. J. Llope,³⁶ R. S. Longacre,³ W. A. Love,³ Y. Lu,³⁸ T. Ludlam,³ G. L. Ma,⁴⁰ Y. G. Ma,⁴⁰ D. P. Mahapatra,¹³ R. Majka,⁵² O. I. Mall,⁵ L. K. Mangotra,¹⁷ R. Manweiler,⁴⁶ S. Margetis,¹⁸ C. Markert,⁴³ H. S. Matis,²¹ Yu. A. Matulenko,³² D. McDonald,³⁶ T. S. McShane,⁹ A. Meschanin,³² R. Milner,²² N. G. Minaev,³² S. Mioduszewski,⁴² A. Mischke,²⁷ B. Mohanty,⁴⁷ D. A. Morozov,³² M. G. Munhoz,³⁷ B. K. Nandi,¹⁴ C. Natrass,⁵² T. K. Nayak,⁴⁷ J. M. Nelson,² P. K. Netrakanti,³³ M. J. Ng,⁴ L. V. Nogach,³² S. B. Nurushev,³² G. Odyniec,²¹ A. Ogawa,³ H. Okada,³ V. Okorokov,²⁵ D. Olson,²¹ M. Pachr,¹⁰ B. S. Page,¹⁵ S. K. Pal,⁴⁷ Y. Pandit,¹⁸ Y. Panebratsev,¹¹ T. Pawlak,⁴⁸ T. Peitzmann,²⁷ V. Perevoztchikov,³ C. Perkins,⁴ W. Peryt,⁴⁸ S. C. Phatak,¹³ P. Pile,³ M. Planinic,⁵³ J. Pluta,⁴⁸ D. Plyku,²⁹ N. Poljak,⁵³ A. M. Poskanzer,²¹ B. V. K. S. Potukuchi,¹⁷ D. Prindle,⁴⁹ C. Pruneau,⁵⁰ N. K. Pruthi,³⁰ P. R. Pujahari,¹⁴ J. Putschke,⁵² R. Raniwala,³⁵ S. Raniwala,³⁵ R. L. Ray,⁴³ R. Redwine,²² R. Reed,⁵ A. Ridiger,²⁵ H. G. Ritter,²¹ J. B. Roberts,³⁶ O. V. Rogachevskiy,¹¹ J. L. Romero,⁵ A. Rose,²¹ C. Roy,⁴¹ L. Ruan,³ M. J. Russcher,²⁷ R. Sahoo,⁴¹ I. Sakrejda,²¹ T. Sakuma,²² S. Salur,²¹ J. Sandweiss,⁵² M. Sarsour,⁴² J. Schambach,⁴³ R. P. Scharenberg,³³ N. Schmitz,²³ J. Seger,⁹ I. Selyuzhenkov,¹⁵ P. Seyboth,²³ A. Shabetai,¹⁶ E. Shahaliev,¹¹ M. Shao,³⁸ M. Sharma,⁵⁰ S. S. Shi,⁵¹ X-H. Shi,⁴⁰ E. P. Sichtermann,²¹ F. Simon,²³ R. N. Singaraju,⁴⁷ M. J. Skoby,³³ N. Smirnov,⁵² R. Snellings,²⁷ P. Sorensen,³ J. Sowinski,¹⁵ H. M. Spinka,¹ B. Srivastava,³³ A. Stadnik,¹¹ T. D. S. Stanislaus,⁴⁶ D. Staszak,⁶ M. Strikhanov,²⁵ B. Stringfellow,³³ A. A. P. Suaide,³⁷ M. C. Suarez,⁸ N. L. Subba,¹⁸ M. Sumera,¹⁰ X. M. Sun,²¹ Y. Sun,³⁸ Z. Sun,²⁰ B. Surrow,²² T. J. M. Symons,²¹ A. Szanto de Toledo,³⁷ J. Takahashi,⁷ A. H. Tang,³ Z. Tang,³⁸ L. H. Tarini,⁵⁰ T. Tarnowsky,²⁴ D. Thein,⁴³ J. H. Thomas,²¹ J. Tian,⁴⁰ A. R. Timmins,⁵⁰ S. Timoshenko,²⁵ D. Tlusty,¹⁰ M. Tokarev,¹¹ T. A. Trainor,⁴⁹ V. N. Tram,²¹ A. L. Trattner,⁴ S. Trentalange,⁶ R. E. Tribble,⁴² O. D. Tsai,⁶ J. Ulery,³³ T. Ullrich,³ D. G. Underwood,¹ G. Van Buren,³ M. van Leeuwen,²⁷ A. M. Vander Molen,²⁴ J. A. Vanfossen, Jr.,¹⁸ R. Varma,¹⁴ G. M. S. Vasconcelos,⁷ I. M. Vasilevski,¹² A. N. Vasiliev,³² F. Videbaek,³ S. E. Vigdor,¹⁵ Y. P. Vijoyi,¹³ S. Vokal,¹¹ S. A. Voloshin,⁵⁰ M. Wada,⁴³ M. Walker,²² F. Wang,³³ G. Wang,⁶ J. S. Wang,²⁰ Q. Wang,³³ X. Wang,⁴⁴ X. L. Wang,³⁸ Y. Wang,⁴⁴

G. Webb,¹⁹ J. C. Webb,⁴⁶ G. D. Westfall,²⁴ C. Whitten Jr.,⁶ H. Wieman,²¹ S. W. Wissink,¹⁵ R. Witt,⁴⁵ Y. Wu,⁵¹ W. Xie,³³ N. Xu,²¹ Q. H. Xu,³⁹ Y. Xu,³⁸ Z. Xu,³ Y. Yang,²⁰ P. Yepes,³⁶ K. Yip,³ I-K. Yoo,³⁴ Q. Yue,⁴⁴ M. Zawisza,⁴⁸ H. Zbroszczyk,⁴⁸ W. Zhan,²⁰ S. Zhang,⁴⁰ W. M. Zhang,¹⁸ X. P. Zhang,²¹ Y. Zhang,²¹ Z. P. Zhang,³⁸ Y. Zhao,³⁸ C. Zhong,⁴⁰ J. Zhou,³⁶ R. Zoulkarneev,¹² Y. Zoulkarneeva,¹² and J. X. Zuo⁴⁰

(STAR Collaboration)

- ¹Argonne National Laboratory, Argonne, Illinois 60439, USA
²University of Birmingham, Birmingham, United Kingdom
³Brookhaven National Laboratory, Upton, New York 11973, USA
⁴University of California, Berkeley, California 94720, USA
⁵University of California, Davis, California 95616, USA
⁶University of California, Los Angeles, California 90095, USA
⁷Universidade Estadual de Campinas, Sao Paulo, Brazil
⁸University of Illinois at Chicago, Chicago, Illinois 60607, USA
⁹Creighton University, Omaha, Nebraska 68178, USA
¹⁰Nuclear Physics Institute AS CR, 250 68 Řež/Prague, Czech Republic
¹¹Laboratory for High Energy (JINR), Dubna, Russia
¹²Particle Physics Laboratory (JINR), Dubna, Russia
¹³Institute of Physics, Bhubaneswar 751005, India
¹⁴Indian Institute of Technology, Mumbai, India
¹⁵Indiana University, Bloomington, Indiana 47408, USA
¹⁶Institut de Recherches Subatomiques, Strasbourg, France
¹⁷University of Jammu, Jammu 180001, India
¹⁸Kent State University, Kent, Ohio 44242, USA
¹⁹University of Kentucky, Lexington, Kentucky, 40506-0055, USA
²⁰Institute of Modern Physics, Lanzhou, China
²¹Lawrence Berkeley National Laboratory, Berkeley, California 94720, USA
²²Massachusetts Institute of Technology, Cambridge, MA 02139-4307, USA
²³Max-Planck-Institut für Physik, Munich, Germany
²⁴Michigan State University, East Lansing, Michigan 48824, USA
²⁵Moscow Engineering Physics Institute, Moscow Russia
²⁶City College of New York, New York City, New York 10031, USA
²⁷NIKHEF and Utrecht University, Amsterdam, The Netherlands
²⁸Ohio State University, Columbus, Ohio 43210, USA
²⁹Old Dominion University, Norfolk, VA, 23529, USA
³⁰Panjab University, Chandigarh 160014, India
³¹Pennsylvania State University, University Park, Pennsylvania 16802, USA
³²Institute of High Energy Physics, Protvino, Russia
³³Purdue University, West Lafayette, Indiana 47907, USA
³⁴Pusan National University, Pusan, Republic of Korea
³⁵University of Rajasthan, Jaipur 302004, India
³⁶Rice University, Houston, Texas 77251, USA
³⁷Universidade de Sao Paulo, Sao Paulo, Brazil
³⁸University of Science & Technology of China, Hefei 230026, China
³⁹Shandong University, Jinan, Shandong 250100, China
⁴⁰Shanghai Institute of Applied Physics, Shanghai 201800, China
⁴¹SUBATECH, Nantes, France
⁴²Texas A&M University, College Station, Texas 77843, USA
⁴³University of Texas, Austin, Texas 78712, USA
⁴⁴Tsinghua University, Beijing 100084, China
⁴⁵United States Naval Academy, Annapolis, MD 21402, USA
⁴⁶Valparaiso University, Valparaiso, Indiana 46383, USA
⁴⁷Variable Energy Cyclotron Centre, Kolkata 700064, India
⁴⁸Warsaw University of Technology, Warsaw, Poland
⁴⁹University of Washington, Seattle, Washington 98195, USA
⁵⁰Wayne State University, Detroit, Michigan 48201, USA
⁵¹Institute of Particle Physics, CCNU (HZNU), Wuhan 430079, China
⁵²Yale University, New Haven, Connecticut 06520, USA
⁵³University of Zagreb, Zagreb, HR-10002, Croatia

(Dated: October 26, 2018)

The STAR collaboration at RHIC presents measurements of $J/\psi \rightarrow e^+e^-$ at mid-rapidity and high transverse momentum ($p_T > 5$ GeV/c) in $p+p$ and central Cu+Cu collisions at $\sqrt{s_{NN}} = 200$ GeV.

The inclusive J/ψ production cross section for Cu+Cu collisions is found to be consistent at high p_T with the binary collision-scaled cross section for $p+p$ collisions, in contrast to previous measurements at lower p_T , where a suppression of J/ψ production is observed relative to the expectation from binary scaling. Azimuthal correlations of J/ψ with charged hadrons in $p+p$ collisions provide an estimate of the contribution of B -meson decays to J/ψ production of $13\% \pm 5\%$.

PACS numbers: 12.38.Mh, 14.40.Gx, 25.75.Dw, 25.75.Nq

Suppression of the $c\bar{c}$ bound state J/ψ meson production in relativistic heavy-ion collisions arising from J/ψ dissociation due to screening of the $c\bar{c}$ binding potential in the deconfined medium has been proposed as a signature of Quark-Gluon Plasma (QGP) formation [1]. Measurements at $\sqrt{s_{NN}} = 17.3$ GeV at the CERN-SPS observed a strong suppression of J/ψ production in heavy-ion collisions [2], although the magnitude of the suppression decreases with increasing J/ψ p_T . This systematic dependence may be explained by initial state scattering (Cronin effect [3]), as well as the combined effects of finite J/ψ formation time and the finite space-time extent of the hot, dense volume where the dissociation can occur [4].

At higher beam energy ($\sqrt{s_{NN}} = 200$ GeV), the PHENIX collaboration at RHIC has measured J/ψ suppression for $p_T < 5$ GeV/ c in central (small impact parameter) Au+Au and Cu+Cu collisions [5] that is similar in magnitude to that observed at the CERN-SPS. This similarity is surprising in light of the expectation that the energy density is significantly higher at larger collision energy. It may be due to the counterbalancing of larger dissociation with recombination of unassociated c and \bar{c} in the medium, which are more abundant at higher energy [6, 7, 8, 9, 10].

Measurements of open heavy-flavor production may also shed light on J/ψ suppression mechanisms. Non-photonic electrons from the semi-leptonic decay of heavy flavor mesons are found to be strongly suppressed in heavy-ion relative to $p+p$ collisions at RHIC [11, 12], an effect that has been attributed to partonic energy loss in dense matter [13]. This process may also contribute to high- p_T J/ψ suppression, if J/ψ formation proceeds through a channel carrying color.

The medium generated in RHIC heavy-ion collisions is thought to be strongly coupled [14], making accurate QCD calculations of quarkonium propagation difficult. The AdS/CFT duality for QCD-like theories may provide insight into heavy fermion pair propagation in a strongly coupled liquid. One such calculation predicts that the dissociation temperature decreases with increasing J/ψ p_T (or velocity) [15]. The temperature achieved at RHIC (~ 1.5 T $_c$) [14] is below this dissociation temperature at low J/ψ p_T , and above it at $p_T \gtrsim 5$ GeV/ c . Consequently, J/ψ production is predicted to be more suppressed at high p_T , in contrast to the standard suppression mechanism. This prediction can be tested with measurements of J/ψ over a broad kinematic range, in

both $p+p$ and nuclear collisions.

The interpretation of J/ψ suppression observed at the SPS and by the PHENIX collaboration requires understanding of the quarkonium production mechanism in hadronic collisions, which include direct production via gluon fusion and color-octet (CO) and color-singlet (CS) transitions, as described by Non-Relativistic Quantum ChromoDynamics (NRQCD) [16]; parton fragmentation; and feeddown from higher charmonium states (χ_c , $\psi(2S)$) and B meson decays. No model at present fully explains the J/ψ systematics observed in elementary collisions [17]. J/ψ measurements at high- p_T both in $p+p$ and nuclear collisions may provide additional insights into the basic processes underlying quarkonium production.

This letter reports new measurements by the STAR collaboration at RHIC of J/ψ production at high transverse momentum in $p+p$ and Cu+Cu collisions at $\sqrt{s_{NN}} = 200$ GeV [18]. The inclusive cross section and semi-inclusive J/ψ -hadron correlations are presented.

The Cu+Cu data are from the RHIC 2005 run, while the $p+p$ data are from 2005 and 2006. The online trigger, utilizing the STAR Barrel Electromagnetic Calorimeter (BEMC) [19] as well as other trigger detectors, required one BEMC tower with an energy deposition above a given threshold in coincidence with a minimum bias (MB) collision trigger [20]. The online trigger threshold, MB trigger condition, and sampled integrated luminosity for each dataset are listed in Tab. I. In Cu+Cu data, the most central 0-20% and 0-60% of the total hadronic cross section were selected as in [20, 21].

In this analysis, $J/\psi \rightarrow e^+e^-$ (Branching Ratio (B)=5.9%) was reconstructed using the STAR Time Projection Chamber (TPC) [22] and BEMC, with acceptance $|\eta| < 1$ and full azimuthal coverage. Hadron rejection was achieved through the combination of BEMC shower energy, shower shape measured in the embedded Shower-Maximum Detector (SMD), and ionization loss (dE/dx) in the TPC [11, 23]. Electron purity is $> 70\%$ with high efficiency. At moderate p_T , the TPC alone can measure electrons with efficiency $> 90\%$ and sufficient hadron rejection ($\sim 10^3$) [11, 24].

Figure 1 shows di-electron invariant mass distributions for (a) $p+p$ and (b) Cu+Cu collisions at $\sqrt{s_{NN}} = 200$ GeV. The like-sign distribution measures random pair background from Dalitz decays and photon conversions. The J/ψ mass window is $2.7 < M_{inv}^{ee} < 3.2$ GeV/ c^2 . Other correlated e^+e^- background is estimated to be $<$

TABLE I: Trigger conditions, off-line cuts and J/ψ signal statistics. E_T is the BEMC trigger threshold. p_{T1} and p_{T2} are the lower bounds for the two electron candidates. BBC (ZDC) means the coincidence of Beam Beam Counters (Zero Degree Calorimeters). S/B is the ratio of signal to background.

	$p+p$ (2005)	$p+p$ (2006)	Cu+Cu
MB trigger	BBC	BBC	ZDC
E_T (GeV)	> 3.5	> 5.4	> 3.75
Sampled int. lumi	2.8 pb^{-1}	11.3 pb^{-1}	$860 \mu\text{b}^{-1}$
p_{T1} (GeV/c)	> 2.5	> 4.0	> 3.5
p_{T2} (GeV/c)	> 1.2	> 1.2	> 1.5
J/ψ p_T (GeV/c)	5-8	5-14	5-8
J/ψ counts	32 ± 6	51 ± 10	23 ± 8
S/B	9:1	2:1	1:4

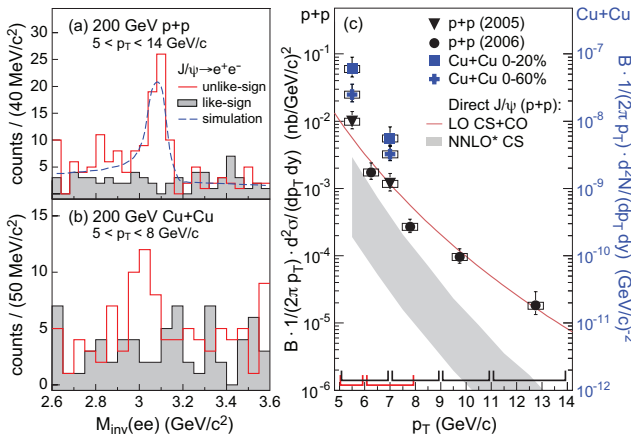


FIG. 1: (Color online.) Left: invariant dielectron mass distribution in (a) $p+p$ and (b) Cu+Cu collisions, for opposite sign (solid red) and same sign pairs (grey band) from data, and simulated J/ψ peak for $p+p$ (dashed). Right: J/ψ p_T distributions in $p+p$ and Cu+Cu collisions at $\sqrt{s_{NN}} = 200$ GeV. Horizontal brackets show bin limits. Also shown are perturbative calculations for LO CS+CO (solid line) and NNLO* CS (band) direct yields, without feeddown contributions.

10% [25, 26, 27]. Table I lists the offline cuts and J/ψ signal statistics. Different thresholds were used for the two electron candidates, corresponding to different online trigger thresholds.

The J/ψ detection efficiency was calculated by two complementary methods. The first method was to determine the electron trigger efficiency by comparing triggered electron yield to the measured inclusive electron spectrum [11]. The non-triggered electron efficiency depends only on the TPC tracking efficiency, which was determined by embedding simulated electron tracks into real events [20], and dE/dx efficiencies, determined from the distributions in real data [23]. The second method was to simulate J/ψ events in PYTHIA [28], embed them into real events, and reconstruct the hybrid event to determine the J/ψ trigger and detection efficiencies. The

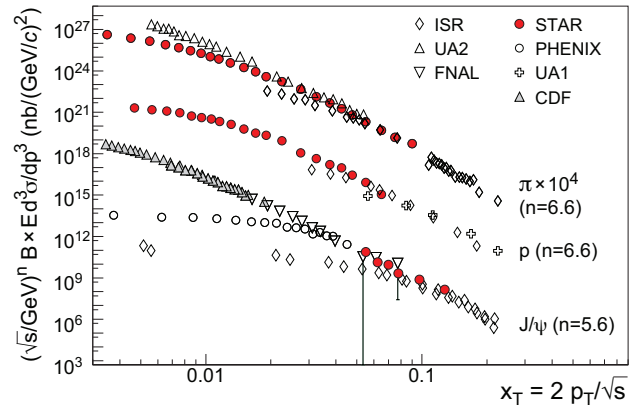


FIG. 2: x_T distributions of pions and protons [33, 34, 35, 36, 37] and J/ψ (CDF [26, 27], UA1 [38], PHENIX [25], and ISR [39]).

difference in estimated efficiency between the two methods is $< 10\%$ for all datasets and is included into the systematic uncertainties of the inclusive spectra. This systematic uncertainty is correlated in $p+p$ and Cu+Cu. A log-likelihood method is used to correct the J/ψ efficiency and calculate the yields [29].

Figure 1 (c) shows the measured $J/\psi \rightarrow e^+e^-$ p_T spectra. The systematic uncertainties are dominated by kinematic cuts, trigger efficiency (9%) and reconstruction efficiency (8%), and are similar and correlated in $p+p$ and Cu+Cu. The normalization uncertainty for the inclusive non-singly diffractive $p+p$ cross section is 14% [30]. Theoretical calculations shown in the figure are NRQCD from CO and CS transitions for direct J/ψ 's in $p+p$ collisions [31] (solid line) and NNLO* CS result [32] (grey band). Neither calculation includes feeddown contributions. The band for NNLO* gives the uncertainty due to scale parameters and the charm quark mass. The CS+CO calculation describes the data well and leaves little room for feeddown from ψ' , χ_c and B , estimated to be a factor of ~ 1.5 . NNLO* CS predicts a steeper p_T dependence.

Proton and pion inclusive production cross sections in high energy $p+p$ collisions have been found to follow x_T scaling [40, 41, 42]: $E \frac{d^3\sigma}{dp^3} = g(x_T)/s^{n/2}$, where $x_T = 2p_T/\sqrt{s}$. In the parton model, n reflects the number of constituents taking an active role in hadron production. Figure 2 shows the x_T distributions of this data and previous J/ψ , pion and proton data, from $p+p$ collisions. The J/ψ data [25, 26, 27, 38, 39] cover the range $\sqrt{s} = 30$ GeV to $\sqrt{s} = 1.96$ TeV. The J/ψ exhibits x_T scaling ($n = 5.6 \pm 0.2$) at high p_T , similar to the trend for pions and protons ($n = 6.6 \pm 0.1$) [34, 35]. While low p_T J/ψ production originates in a hard process due to the mass scale, subsequent soft processes could cause violation of x_T scaling. At high p_T , the power parameter $n = 5.6 \pm 0.2$ is closer to the predictions from CO

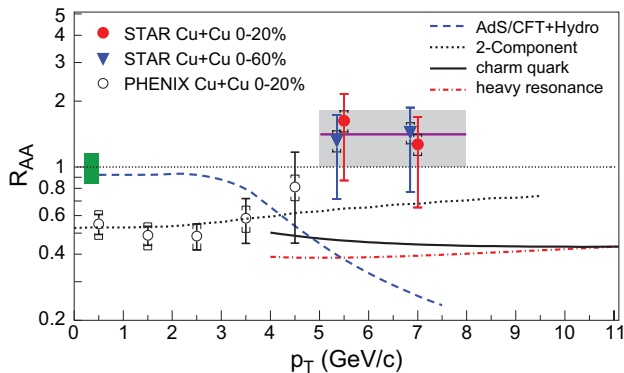


FIG. 3: (Color online). J/ψ R_{AA} vs. p_T . STAR data points have statistical (bars) and systematic (caps) uncertainties. The box about unity on the left shows R_{AA} normalization uncertainty, which is the quadrature sum of p+p normalization and binary collision scaling uncertainties. The solid line and band show the average and uncertainty of the two 0-20% data points. The curves are model calculations described in the text. The uncertainty band of 10% for the dotted curve is not shown.

and Color-Evaporation production ($n \simeq 6$) [31, 43] and much smaller than that from next-to-next-to leading order (NNLO*) CS production ($n \simeq 8$) [32]. This is also evident from Fig. 1 (c).

The nuclear modification factor $R_{AA}(p_T)$ [44], defined as the ratio of the inclusive hadron yield in nuclear collisions to that in $p+p$ collisions scaled by the underlying number of binary nucleon-nucleon collisions, measures medium-induced effects on inclusive particle production. In the absence of such effects, R_{AA} is unity for hard processes.

Figure 3 shows R_{AA} for J/ψ vs p_T , in 0-20% Cu+Cu collisions from PHENIX [45] and STAR, and 0-60% Cu+Cu from STAR. Cu+Cu and $p+p$ data with $p_T > 5$ GeV/c are from STAR. The R_{AA} systematic uncertainty takes into account the correlated efficiencies of the Cu+Cu and $p+p$ datasets. R_{AA} for J/ψ is seen to increase with increasing p_T . The average of the two STAR 0-20% data points at high- p_T is $R_{AA} = 1.4 \pm 0.4$ (*stat.*) ± 0.2 (*syst.*). Utilizing the STAR Cu+Cu and $p+p$ data reported here and PHENIX Cu+Cu data at high- p_T [45] gives $R_{AA} = 1.1 \pm 0.3$ (*stat.*) ± 0.2 (*syst.*) for $p_T > 5$ GeV/c. Both results are consistent with unity and differ by two standard deviations from a PHENIX measurement at lower p_T ($R_{AA} = 0.52 \pm 0.05$ [45]). A notable conclusion from these data is that J/ψ is the only hadron measured in RHIC heavy-ion collisions that does not exhibit significant high p_T suppression. However, for the J/ψ population reported here, the initial scattered partons have average momentum fraction ~ 0.1 (see also Fig. 2), where initial state effects such as anti-shadowing may lead to increasing R_{AA} with increasing p_T .

The dashed curve in Fig. 3 shows the prediction of

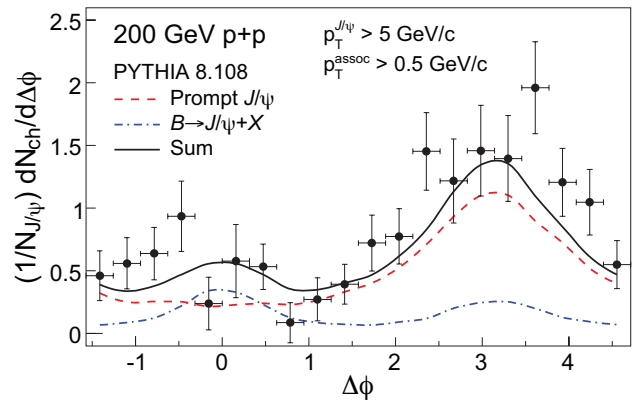


FIG. 4: (Color online). J/ψ -hadron azimuthal correlations. Lines show PYTHIA calculation of prompt (dashed) and B -meson (dot-dashed) feeddown contributions, and their sum (solid).

an AdS/CFT-based calculation, in which the J/ψ is embedded in a hydrodynamic model [46] and the J/ψ dissociation temperature decreases with increasing velocity according to [15]. Its p_T dependence is at variance with that of the data. The dotted line shows the prediction of a two-component model including color screening, hadronic phase dissociation, statistical $c\bar{c}$ coalescence at the hadronization transition, J/ψ formation time effects, and B -meson feeddown [3]. This calculation describes the overall trend of the data.

The other calculations in Fig. 3 provide a comparison to open charm R_{AA} . The solid line is based on the WHDG model for charm quark energy loss, with assumed medium gluon density $dN_g/dy = 254$ for 0-20% Cu+Cu [47]. The dash-dotted line shows a GLV model calculation for D-meson energy loss, with $dN_g/dy = 275$ [48]. Both models, which correctly describe heavy-flavor suppression in Au+Au collisions, predict charm meson suppression of a factor ~ 2 at $p_T > 5$ GeV/c. This is in contrast to the J/ψ R_{AA} . This comparison suggests that high- p_T J/ψ production does not proceed dominantly via a channel carrying color. However, other effects [3, 49] may compensate for the predicted loss in this p_T range.

Figure 4 shows the azimuthal correlation between high- p_T J/ψ ($p_T > 5$ GeV/c) and charged hadrons with $p_T > 0.5$ GeV/c in 200 GeV $p+p$ collisions. The J/ψ mass window is narrowed to 2.9-3.2 GeV/ c^2 to increase the S/B ratio. There is no significant correlated yield in the near-side ($\Delta\phi \sim 0$), in contrast to dihadron correlation measurements [50]. The lines show the result of a PYTHIA calculation [28], which exhibits a near-side correlation due dominantly to $B \rightarrow J/\psi + X$. A χ^2 fit to the data of the summed distribution (directly produced J/ψ , feeddown from χ_c , $\psi(2S)$ and B -meson) gives a contribution from B -meson feeddown to inclusive J/ψ production of $13\% \pm 5\%$ at $p_T > 5$ GeV/c.

In summary, we report new measurements of J/ψ pro-

duction in $\sqrt{s} = 200$ GeV $p+p$ and Cu+Cu collisions at high p_T ($p_T > 5$ GeV/ c) at RHIC. The J/ψ inclusive cross section was found to obey x_T scaling for $p_T \gtrsim 5$ GeV/ c , in contrast to lower p_T J/ψ production. The J/ψ nuclear modification factor R_{AA} in Cu+Cu increases from low to high p_T and is consistent with no J/ψ suppression for $p_T > 5$ GeV/ c , in contrast to the prediction from a theoretical model of quarkonium dissociation in a strongly coupled liquid using an AdS/CFT approach. The two-component model with finite J/ψ formation time describes the increasing trend of the J/ψ R_{AA} . Based on the measurement of azimuthal correlations and the comparison to model calculations, we estimate the fraction of J/ψ from B -meson decay to be $13 \pm 5\%$ at $p_T > 5$ GeV/ c .

The authors thank G.C. Nayak, J.P. Lansberg, W.A. Horowitz and I. Vitev for providing calculations and discussion. We thank the RHIC Operations Group and RCF at BNL, and the NERSC Center at LBNL and the resources provided by the Open Science Grid consortium for their support. This work was supported in part by the Offices of NP and HEP within the U.S. DOE Office of Science, the U.S. NSF, the Sloan Foundation, the DFG Excellence Cluster EXC153 of Germany, CNRS/IN2P3, RA, RPL, and EMN of France, STFC and EPSRC of the United Kingdom, FAPESP of Brazil, the Russian Ministry of Sci. and Tech., the NNSFC, CAS, MoST, and MoE of China, IRP and GA of the Czech Republic, FOM of the Netherlands, DAE, DST, and CSIR of the Government of India, the Polish State Committee for Scientific Research, and the Korea Sci. & Eng. Foundation.

-
- [1] T. Matsui and H. Satz, Phys. Lett. **B178**, 416 (1986).
 [2] M. C. Abreu et al., Phys. Lett. **B499**, 85 (2001).
 [3] X. Zhao and R. Rapp (2007), arXiv:0712.2407.
 [4] F. Karsch and R. Petronzio, Phys. Lett. **B212**, 255 (1988).
 [5] A. Adare et al., Phys. Rev. Lett. **98**, 232301 (2007).
 [6] P. Braun-Munzinger and J. Stachel, Phys. Lett. **B490**, 196 (2000).
 [7] L. Grandchamp and R. Rapp, Phys. Lett. **B523**, 60 (2001).
 [8] M. I. Gorenstein et al., Phys. Lett. **B524**, 265 (2002).
 [9] R. L. Thews, M. Schroedter, and J. Rafelski, Phys. Rev. **C63**, 054905 (2001).
 [10] A. D. Frawley, T. Ullrich, and R. Vogt, Phys. Rept. **462**, 125 (2008).
 [11] B. I. Abelev et al., Phys. Rev. Lett. **98**, 192301 (2007).
 [12] A. Adare et al., Phys. Rev. Lett. **98**, 172301 (2007).
 [13] Y. L. Dokshitzer and D. E. Kharzeev, Phys. Lett. **B519**, 199 (2001).
 [14] J. Adams et al., Nucl. Phys. **A757**, 102 (2005).
 [15] H. Liu, K. Rajagopal, and U.A. Wiedemann, Phys. Rev. Lett. **98**, 182301 (2007).
 [16] G. T. Bodwin, E. Braaten, and G. P. Lepage, Phys. Rev. **D51**, 1125 (1995), hep-ph/9407339.
 [17] N. Brambilla et al. (2004), hep-ph/0412158.
 [18] K. H. Ackermann et al., Nucl. Instrum. Meth. **A499**, 624 (2003).
 [19] M. Beddo et al., Nucl. Instrum. Meth. **A499**, 725 (2003).
 [20] B. I. Abelev et al. (2008), arXiv:0808.2041.
 [21] B. I. Abelev et al. (2008), arXiv:0810.4979.
 [22] M. Anderson et al., Nucl. Instrum. Meth. **A499**, 659 (2003).
 [23] Y.-C. Xu et al. (2008), arXiv:0807.4303.
 [24] J. Adams et al., Phys. Rev. Lett. **94**, 062301 (2005).
 [25] A. Adare et al., Phys. Rev. Lett. **98**, 232002 (2007).
 [26] F. Abe et al., Phys. Rev. Lett. **79**, 572 (1997).
 [27] D. E. Acosta et al., Phys. Rev. **D71**, 032001 (2005).
 [28] T. Sjostrand, S. Mrenna, and P. Skands, JHEP **05**, 026 (2006).
 [29] Z. Tang, Ph.D. thesis, University of Science and Technology and China (2009).
 [30] J. Adams et al., Phys. Rev. Lett. **91**, 172302 (2003).
 [31] G. C. Nayak, M. X. Liu, and F. Cooper, Phys. Rev. **D68**, 034003 (2003), and private communication.
 [32] P. Artoisenet et al., Phys. Rev. Lett. **101**, 152001 (2008), and J.P. Lansberg private communication.
 [33] M. Banner et al., Phys. Lett. **B115**, 59 (1982).
 [34] J. Adams et al., Phys. Lett. **B637**, 161 (2006).
 [35] J. Adams et al., Phys. Lett. **B616**, 8 (2005).
 [36] B. Alper et al., Nucl. Phys. **B100**, 237 (1975).
 [37] D. Antreasyan et al., Phys. Rev. **D19**, 764 (1979).
 [38] C. Albajar et al., Phys. Lett. **B256**, 112 (1991).
 [39] C. Kourkoumelis et al., Phys. Lett. **B91**, 481 (1980).
 [40] A. G. Clark et al., Phys. Lett. **B74**, 267 (1978).
 [41] A. L. S. Angelis et al., Phys. Lett. **B79**, 505 (1978).
 [42] S. S. Adler et al., Phys. Rev. **C69**, 034910 (2004).
 [43] M. Bedjidian et al. (2004), and R. Vogt private communication.
 [44] C. Adler et al., Phys. Rev. Lett. **89**, 202301 (2002).
 [45] A. Adare et al., Phys. Rev. Lett. **101**, 122301 (2008).
 [46] T. Gunji, J. Phys.G: Nucl. Part. Phys. **35**, 104137 (2008).
 [47] S. Wicks et al., Nucl. Phys. **A784**, 426 (2007), and W. A. Horowitz private communication.
 [48] A. Adil and I. Vitev, Phys. Lett. **B649**, 139 (2007), and I. Vitev private communication.
 [49] X.-M. Xu, Nucl. Phys. **A697**, 825 (2002).
 [50] J. Adams et al., Phys. Rev. Lett. **95**, 152301 (2005).